



INSTITUT DE FRANCE
Académie des sciences

Comptes Rendus

Chimie

Manel Hanana, Christophe Kahlfuss, Jean Weiss, Renaud Cornut,
Bruno Jousselve, Jennifer A. Wytko and Stéphane Campidelli

**ORR activity of metalated phenanthroline-strapped porphyrin adsorbed
on carbon nanotubes**

Volume 24, Special Issue S3 (2021), p. 5-12


Published online: 8 June 2021

Issue date: 16 December 2021

<https://doi.org/10.5802/crchim.86>

Part of Special Issue: MAPYRO: the French Fellowship of the Pyrrolic Macrocyclic
Ring

Guest editors: Bernard Boitrel (Institut des Sciences Chimiques de Rennes,
CNRS-Université de Rennes 1, France) and Jean Weiss (Institut de Chimie de
Strasbourg, CNRS-Université de Strasbourg, France)

 This article is licensed under the
CREATIVE COMMONS ATTRIBUTION 4.0 INTERNATIONAL LICENSE.
<http://creativecommons.org/licenses/by/4.0/>



Les Comptes Rendus. Chimie sont membres du
Centre Mersenne pour l'édition scientifique ouverte
www.centre-mersenne.org
e-ISSN : 1878-1543



MAPYRO: the French Fellowship of the Pyrrolic Macrocyclic Ring / *MAPYRO: la communauté française des macrocycles pyrroliques*

ORR activity of metalated phenanthroline-strapped porphyrin adsorbed on carbon nanotubes

Manel Hanana^a, Christophe Kahlfuss^b, Jean Weiss^b, Renaud Cornut^a,
Bruno Jousselme^a, Jennifer A. Wytko^{*,b} and Stéphane Campidelli^{*,a}

^a Université Paris-Saclay, CEA, CNRS, NIMBE, LICSEN, 91191, Gif-sur-Yvette, France

^b Institut de Chimie de Strasbourg, UMR 7177 CNRS-Université de Strasbourg, 4 rue Blaise Pascal, 67008 Strasbourg, France

E-mails: manelhanana@yahoo.fr (M. Hanana), christophe.kahlfuss@gmail.com (C. Kahlfuss), jweiss@unistra.fr (J. Weiss), renaud.cornut@cea.fr (R. Cornut), bruno.jousselme@cea.fr (B. Jousselme), jwytko@unistra.fr (J. A. Wytko), stephane.campidelli@cea.fr (S. Campidelli)

Abstract. Developing efficient noble metal-free systems for electrocatalysis and the reduction of oxygen (ORR) is crucial for hydrogen economy. Bioinspired hybrids combining iron or copper/iron porphyrins with multiwalled carbon nanotubes were tested for ORR using a rotating ring-disk electrode at pH 13 to 8. The porphyrin-nanotube hybrids exhibited better electrocatalytic properties than their constituents alone due to the electrical network formed by the nanotubes, and they reduced oxygen via a four-electron pathway to produce water. Whereas the presence of Cu was not mandatory to reduce oxygen, its presence improved ORR activity and decreased the overpotential compared to monometallic (iron porphyrin) hybrids.

Résumé. La conception de matériaux sans métaux nobles pour la réaction de réduction de l'oxygène (ORR) est cruciale pour le développement d'une économie basée sur l'hydrogène. Ici, des matériaux hybrides bioinspirés à base de porphyrines métallées et de nanotubes de carbone multi-parois ont été testés pour l'ORR avec un système d'électrode disque-anneau entre pH 8 et 13. Les matériaux hybrides présentent systématiquement de meilleures propriétés électrocatalytiques que celles de leurs constituants pris individuellement et permettent de réduire l'oxygène par un processus à quatre électrons. La présence du cuivre dans les hybrides n'est pas obligatoire mais elle améliore légèrement les propriétés électrocatalytiques.

Keywords. Porphyrin, Carbon nanotubes, Oxygen reduction, Electrocatalysis, Energy.

Mots-clés. Porphyrine, Nanotubes de carbone, Réduction de l'oxygène, Électrocatalyse, Énergie.

Available online 8th June 2021

* Corresponding authors.

1. Introduction

For the last decade, the development of non-noble metal or metal-free catalysts for energy sources has been a field of growing interest. The electrocatalytic reduction of oxygen (oxygen reduction reaction—ORR) is the key reaction for the efficiency of fuel cells. Its slow kinetics, multistep process and the competition between the two-electron and four-electron pathway make ORR the limiting reaction in fuel cells. Whereas the best catalysts for this electrocatalytic reaction remain platinum-based materials, in the last ten years, much effort has been devoted to the development of nonprecious metal or metal-free catalysts for ORR [1–15]. In addition, recently, the composition and the morphology of the Fe–N–C active sites in pyrolyzed catalyst materials have been investigated [16–20].

In Nature, the reduction of oxygen is performed by the active center composed of an iron porphyrin and copper-histidine complexes in cytochrome *c* oxidase (CcO). In 1964, Jasinski discovered that a relatively simple macrocycle like cobalt phthalocyanine was able to reduce oxygen [21]. In metalated phthalocyanines, the metal core is coordinated in a plane of four nitrogen atoms bearing a global -2 charge. Consequently, other tetrapyrrolic macrocycles, such as metalated porphyrins, phthalocyanines or corroles, have been extensively studied in the literature as mimics of cytochrome *c* oxidase and/or as catalysts for the reduction of oxygen to water in fuel cells [11–14,22–41]. In these systems, the macrocycle containing an inexpensive metal (mostly Fe or Co) constitutes the active part of the catalyst and the electrons and protons required for the reaction have to be properly delivered to ensure the efficiency of the reduction. However, the electrocatalytic properties of a material appear to be extremely dependent on its environment [37]. In this context, we have systematically investigated the properties of porphyrin and phthalocyanine complexes in the presence of carbon nanotubes as electron transporters and Nafion as proton source [33,34,40,41].

Inspired by Nature, early, elaborate, covalent models of CcO reported by Collman [22,23] and Boitrel [24] are considered as milestones in the design of artificial hemoproteins. These models employed caps and straps that served to differentiate both faces of tetra-aryl-porphyrin derivatives and

to create steric hindrance that mimicked the distal site of the hemoprotein. Over the past years, the properties of a phenanthroline-strapped porphyrin have been exploited in several domains such as the specific recognition of imidazole or the formation of hetero-bimetallic structures containing Fe and Cu for the electrocatalytic reduction of oxygen [42]. In these ditopic ligands, the phenanthroline binds and stabilizes a copper(I) ion at a distance of approximately 4.7 Å from an iron porphyrin, mimicking a heme. In previous studies, these structures, decorated with pendant pyridine or imidazole ligands were evaluated as models of cytochrome *c* oxidase in physiological media [43] (phosphate buffer) but were never studied under the working conditions of a proton exchange membrane fuel-cell (PEMFC). The absorption of phenanthroline-strapped iron (Fe-P) and iron(III)/copper(I) porphyrins (Cu/Fe-P) on multiwalled carbon nanotubes (MWNTs) and their electrocatalytic properties are reported hereafter. These studies demonstrate that the MWNT-Fe-P and Cu/Fe-P hybrids efficiently reduce oxygen *via* a four-electron pathway to yield water. In contrast to our previous work in which a multilayer of porphyrins decorated the nanotube surface [34], here, the presence of the rigid phenanthroline strap on the porphyrin prevents the formation of a multilayer on the MWNTs and the porphyrins likely interact with the nanotubes by π -stacking and C–H– π interactions.

2. Results and discussion

The porphyrin complexes Fe-P and Cu/Fe-P were prepared from the phenanthroline-strapped porphyrin (H₂P) [44] as shown in Scheme 1. Metalation of the porphyrin with FeCl₂ in refluxing DMF afforded Fe-P in 62% yield. The insertion of iron(III) and the presence of an axial chloride on the iron center were confirmed by mass spectrometry. The bimetallic Cu/Fe-P complex was prepared quantitatively by subsequent reaction of Fe-P with [Cu(CH₃CN)₄]PF₆ under inert atmosphere.

The nanotube-porphyrin hybrids were prepared by mixing MWNT with porphyrins Fe-P or Cu/Fe-P (in a 3:1 ratio by weight) in tetrahydrofuran (THF) in an ultrasound bath. It was assumed that the presence of the phenanthroline strap would eliminate stacking and subsequent formation of multilayers on the side-walls of the nanotube. The 3:1 ratio was chosen by

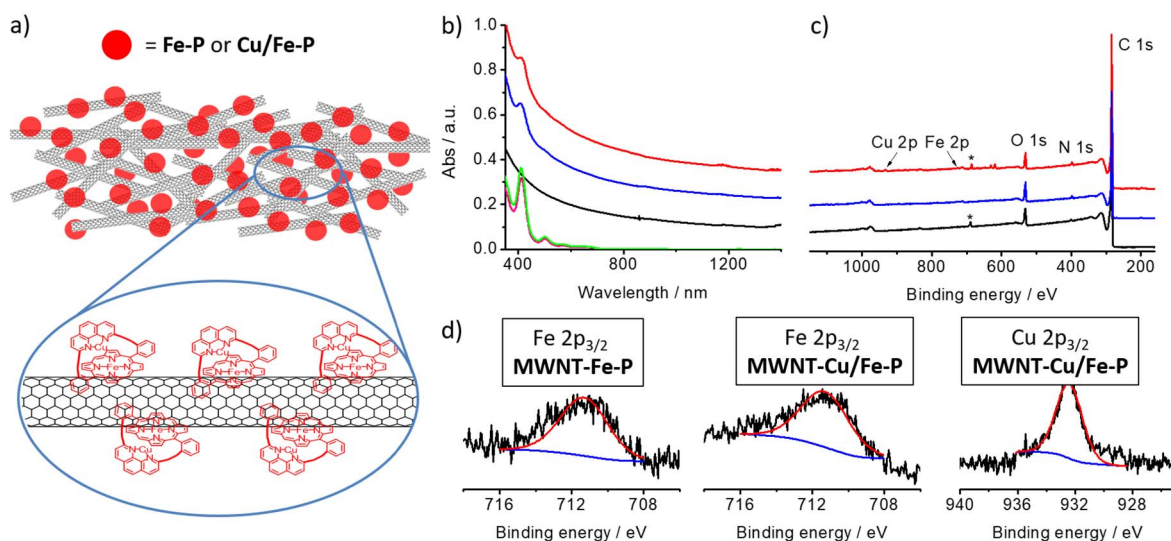
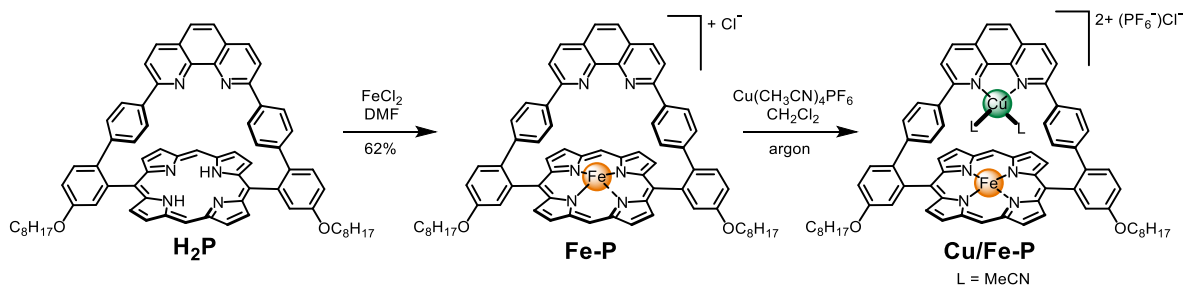


Figure 1. (a) Representation of MWNT-Fe-P and MWNT-Cu/Fe-P hybrids; (b) absorption spectra of Fe-P (pink) and Cu/Fe-P (green) and of MWNT (black), MWNT-Fe-P (blue) and MWNT-Cu/Fe-P (red) recorded in *N*-methylpyrrolidone; (c) XPS Spectra of MWNT (black), MWNT-Fe-P (blue) and MWNT-Cu/Fe-P (red). The signals labeled (*) are due to fluorine from the PTFE membrane. (d) High resolution XPS spectra of Fe $2p_{3/2}$ of MWNT-Fe-P and MWNT-Cu/Fe-P and Cu $2p_{3/2}$ of MWNT-Cu/Fe-P.

assuming that the specific surface area of the MWNTs was *ca.* 320 m²/g [45] and that a porphyrin (without alkyl chains) could be represented by a rectangle of $1.7 \times 0.9 \approx 1.5$ nm². The available surface of 3 mg of nanotubes is estimated to be 1 m² that roughly corresponds to the surface occupied by 1 mg of porphyrin: $m_{\text{porph}}/M_{\text{porph}} \times N_A \times A_{\text{porph}} \approx 0.8$ m².

After mixing, THF was evaporated with a N₂ flow and the catalytic inks were prepared by dispersing by ultrasound sonication the MWNT/porphyrin hybrids (3 mg) of interest in 750 mL of ethanol and 75 mL of Nafion solution (5% in alcohol). Similarly, the inks of the reference compounds MWNT, Fe-P and Cu/Fe-P

were prepared by mixing the nanotubes or the porphyrins in 750 mL of ethanol and 75 mL of Nafion solution (5% in alcohol). The different catalysts and reference materials were drop-casted on a glassy carbon disk and tested in a series of rotating ring-disk electrode (RRDE) experiments at pH 13 (0.1 M NaOH), 10 and 8 (phosphate buffer).

A representation of the nanotube-porphyrin hybrids is shown in Figure 1a and their absorption spectra are given in Figure 1b. The spectra of MWNT-Fe-P and MWNT-Cu/Fe-P are the sum of the absorption of the two counterparts (nanotubes and porphyrins), thus confirming the presence of the porphyrins. The

Table 1. Atomic composition of the MWNT-Fe-P and MWNT-Cu/Fe-P hybrids

	%C	%N	%O	%Fe	%Cu
MWNT-Fe-P	92.22	1.20	6.50	0.09	—
MWNT-Cu/Fe-P	94.09	1.30	4.39	0.11	0.11

hybrids were characterized by absorption and X-ray photoelectron spectroscopies (XPS). The XPS spectra of MWNT, MWNT-Fe-P and MWNT-Cu/Fe-P are shown in Figure 1c. The spectrum of MWNT shows an intense peak of carbon, the presence of oxygen and a small peak at *ca.* 690 eV coming from the PTFE membrane that supports the nanotubes for the analysis. This peak is also observed in the spectrum of MWNT-Cu/Fe-P. The spectra of MWNT-Fe-P and MWNT-Cu/Fe-P show additional peaks attributed to the presence of nitrogen, iron and copper (for MWNT-Cu/Fe-P) (Figure 1d). The extremely weak peaks of iron and copper reflect the low amount of porphyrins absorbed on the nanotubes. The weak signals of the Soret band in the UV-Vis-NIR spectra of MWNT-Fe-P and MWNT-Cu/Fe-P (Figure 1b) also support this observation. The composition of the MWNT-Fe-P and MWNT-Cu/Fe-P determined by XPS is summarized in Table 1. *Note that the percentage of iron and copper must be considered with caution because of the uncertainty of the XPS measurements.*

The redox potentials of the metals in the porphyrins and in the phenanthroline strap were determined by cyclic voltammetry with 1 mM solutions of Fe-P or Cu/Fe-P porphyrin in a 0.1 M tetrabutylammonium hexafluorophosphate (NBu₄PF₆) THF solution. The electrochemical cell was equipped with a glassy carbon working electrode, a platinum counter electrode and an Ag/AgNO₃ (10 mM) reference electrode. The potentials are reported *vs* ferrocene used as internal reference. The solutions were degassed by bubbling argon and the cyclic voltammetry was performed at a scan rate of 20 mV/s. The voltammograms of Fe-P and Cu/Fe-P (Figure S1) show a reversible reduction peak (I) attributed to the first reduction of the porphyrin macrocycles at −1.57 and −1.60 V, respectively. A second more complex signal (II), observed between −0.50 and −0.90 V, is attributed to the reduction of Fe(III)/Fe(II) in the porphyrins. The complex shape of this redox couple associated with this process is attributable to the

presence and exchange of an axial ligand (residual H₂O, a solvent molecule, Cl[−] or no ligand) on the iron(III) center. As previously observed, when copper is present in the phenanthroline strap (Cu/Fe-P), the apical ligand exchange is slow or hindered and can result in an irreversible reduction wave [43,46]. Finally, in the Cu/Fe-P derivative, an additional reversible signal (III) is observed at 0.09 V and corresponds to the oxidation of Cu(I) to Cu(II).

The ORR electrocatalytic properties of two hybrids (MWNT-Fe-P and MWNT-Cu/Fe-P) and of MWNT, Fe-P and Cu/Fe-P used as references, were investigated by rotating ring-disk electrode (RRDE) measurements. Figure 2 presents the ORR activity at different pHs of the catalyst inks deposited on the glassy carbon (GC) electrode (0.196 cm²). The rotating ring electrode (RDE) curves are the average currents calculated from the forward (reduction) and backward (re-oxidation) scans. Figures 2a and b show the polarization curves at 0, 400, 800, 1200, 1600 and 2000 rpm at pH 10 of the MWNT-Fe-P and MWNT-Cu/Fe-P series, respectively. First, the catalyst inks made by mixing the nanotubes with the porphyrins (MWNT-Fe-P and MWNT-Cu/Fe-P) exhibit higher current density and lower overpotential (by about 0.2 V) than Fe-P and Cu/Fe-P alone and also higher current density than bare MWNT. These differences can be explained by the difficulty for electrons to reach the porphyrins embedded in Nafion and by the [2 + 2] electron pathway of the ORR for pure carbon materials [47], respectively. Figures 2c–h show the polarization curves recorded at 800 rpm at different pH, from pH 13 to 8. In all cases, the nanotube/porphyrin hybrids exhibit better ORR properties than the materials (MWNT and Fe-P or Cu/Fe-P) taken separately. The polarization curves of MWNT, Fe-P, Cu/Fe-P, MWNT-Fe-P and MWNT-Cu/Fe-P between 0 and 2000 rpm at pH 13 and 8 are summarized in Figure S2. For all pH considered, Fe-P and Cu/Fe-P alone exhibit an overpotential between 130 to 240 mV (determined for current density at the disk of −0.1 mA·cm^{−2}) compared to the nanotubes hybrids (MWNT-Fe-P and MWNT-Cu/Fe-P). Moreover, on the RDE curves, it is interesting to note that, for the hybrid catalysts, the disk currents reach a plateau, indicating that the reduction of oxygen is limited by diffusion (by the supply of oxygen) and not by the catalyst itself. Finally, comparison of the properties of the monometallic and bimetallic hybrid

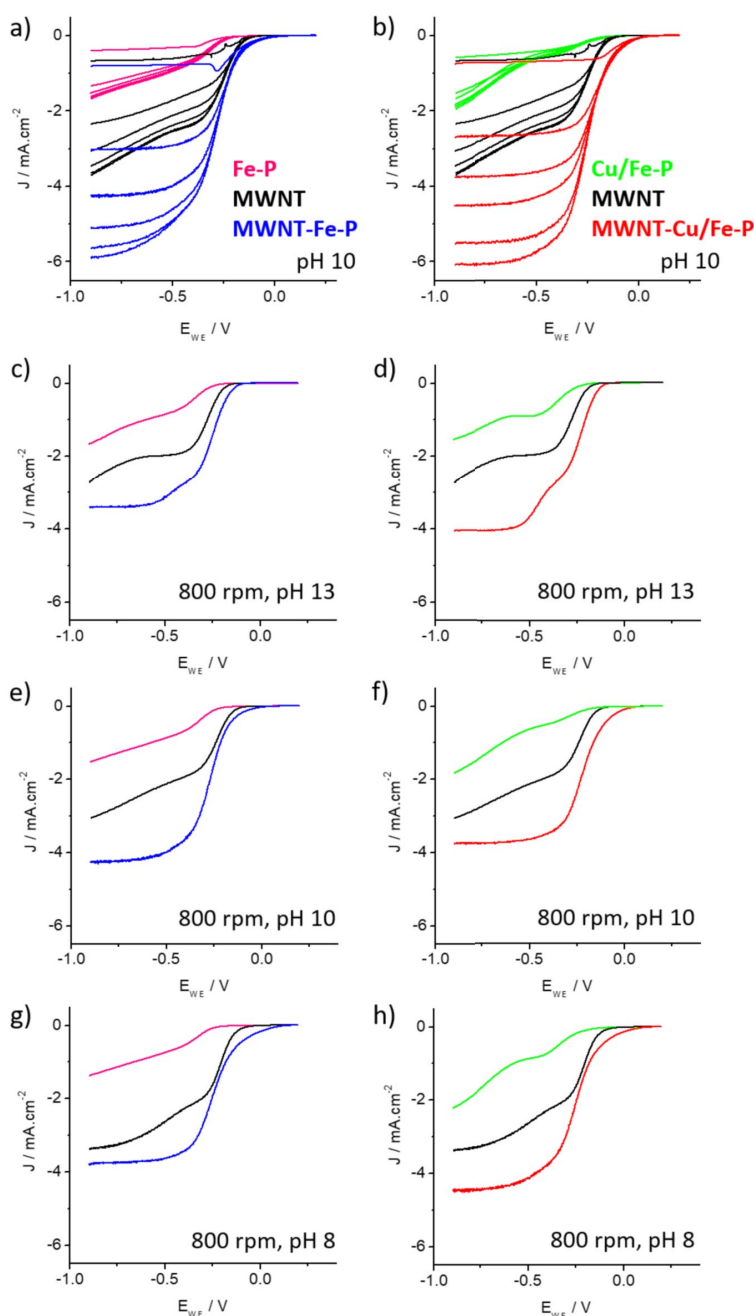


Figure 2. (a, b) Polarization curves at different rotation rates (0, 400, 800, 1200, 1600 and 2000 rpm) for (a) Fe-P (pink curves), MWNT (black curves) and MWNT-Fe-P (blue curves) and for (b) Cu/Fe-P (green curves), MWNT (black curves) and MWNT-Cu/Fe-P (red curves) recorded for ORR in O₂-saturated phosphate buffer solutions at pH 10 (scan rate = 5 mV/s, room temperature). (c, e, g) Polarization curves recorded at different pH at a rotation rate of 800 rpm for Fe-P (pink curves), MWNT (black curves) and MWNT-Fe-P (blue curves). (d, f, h) Polarization curves recorded at different pH at a rotation rate of 800 rpm for Cu/Fe-P (green curves), MWNT (black curves) and MWNT-Cu/Fe-P (red curves).

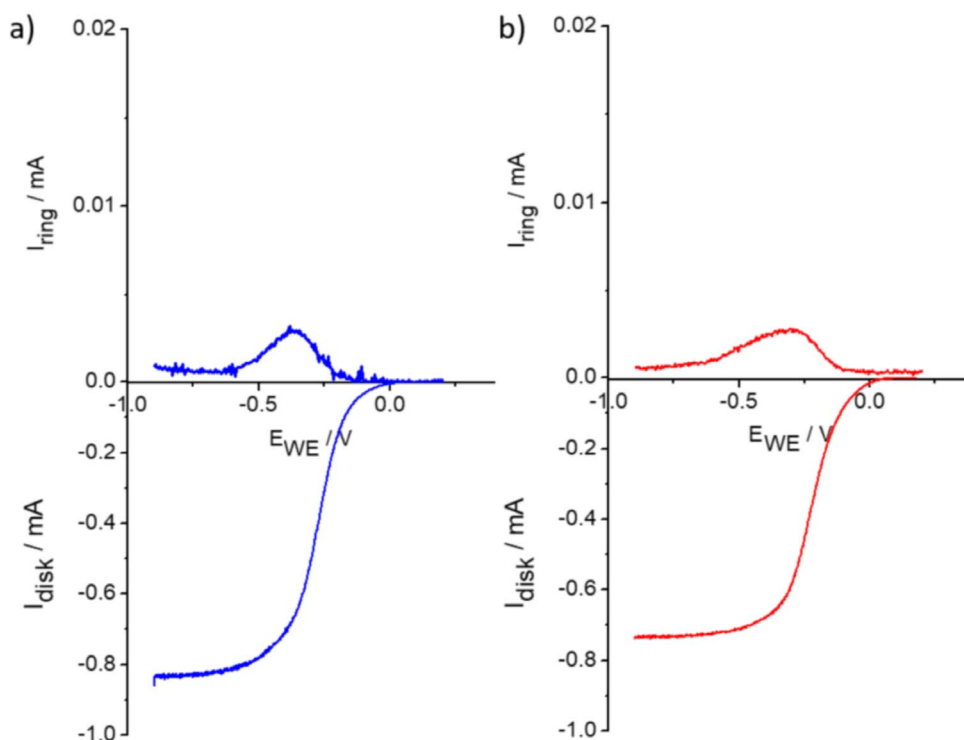


Figure 3. Example RRDE curves with disk and ring currents for (a) MWNT-Fe-P (blue) and (b) MWNT-Cu/Fe-P (red) at pH 10 with a rotation rate of 800 rpm.

catalysts demonstrates that the presence of copper slightly improves the reduction potential and the current density (see Figures 2a, b and S2).

The electrocatalytic properties of Fe-P and Cu/Fe-P and of their nanotube hybrids (MWNT-Fe-P and MWNT-Cu/Fe-P) degrade rapidly in acidic conditions (pH 6 and below—result not shown), thus requiring the deposition of a new catalyst ink for each rotation cycle. This observation is in agreement with our previous report [41] and could be due to demetallation and/or degradation of the porphyrin [48–50]. Therefore, the catalytic properties of these materials in acidic media were not investigated in detail.

The number of electrons involved in the reduction of oxygen was determined from the disk and ring currents at -0.75 V according to the equation: $n = 4I_D / (I_D + I_R/N_c)$ with a collection coefficient $N_c = 0.2$ determined using the one-electron $[\text{Fe}(\text{CN})_6]^{3-}/[\text{Fe}(\text{CN})_6]^{4-}$ redox couple. Figure 3 shows the ring and disk current for MWNT-Fe-P and MWNT-Cu/Fe-P at pH 10 for a rotation rate of 800 rpm; the RRDE curves of the reference materials

MWNT, Fe-P and Cu/Fe-P and those of MWNT-Fe-P and MWNT-Cu/Fe-P at pH 13, 10 and 8 are given in Figure S3. The number of electrons for the reduction of oxygen is reported in Table 2. The RRDE curves (Figures 3 and S3) show that the reduction of O_2 is accompanied by the production of hydrogen peroxide for MWNT, Fe-P and Cu/Fe-P. Conversely, for MWNT-Fe-P and MWNT-Cu/Fe-P, almost no production of H_2O_2 is detected at the plateau and the reduction proceeds *via* a four-electron pathway. As seen in Table 2, in the absence of nanotubes, Cu/Fe-P seems more active in ORR than the copper-free porphyrin Fe-P. In the absence of nanotubes, the limited conductivity of electrons may affect the performance of the monometallic porphyrin. This assumption is supported by a report of Collman [23], which suggests that under limited electron flux, copper and phenol are required to enhance the selective reduction of oxygen to water. In the presence of the nanotubes, the two porphyrins behave similarly and no noticeable differences are observed between MWNT-Fe-P and MWNT-Cu/Fe-P in terms of reduction of

Table 2. Summary of the number of electrons involved in the reduction of oxygen for MWNT, Fe-P, Cu/Fe-P, MWNT-Fe-P and MWNT-Cu/Fe-P

	MWNT	Fe-P	Cu/Fe-P	MWNT-Fe-P	MWNT-Cu/Fe-P
pH 13	3.62	3.08	3.61	3.99	3.98
pH 10	3.86	3.34	3.72	3.98	3.98
pH 8	3.91	3.73	3.95	3.99	3.98

oxygen because MWNTs ensure a sufficient flux of electrons to the iron porphyrin reactive sites for the reduction.

The data in Table 2 are also consistent with previous studies of Fe-P and Cu/Fe-P adsorbed on edge-oriented pyrolytic graphite (EOPG) electrodes [51] and reports by Boitrel and coworkers [24] showing that Fe-porphyrins alone can perform four-electron reduction of oxygen to some extent, possibly due to the presence of face-to-face oriented species.

Beyond their academic interest for the reduction of oxygen, it is clear that carbon nanotube/porphyrin hybrids cannot compete with the performance of platinum-based materials or platinum alloys for PEMFC. However, the recent development of noble metal-free pyrolyzed materials for fuel cells sheds light on the need for comprehensive studies to understand the structures of the ORR active sites. Iron porphyrins combined with nanotubes can play a role in this understanding. Moreover, the combination of the electronic properties of the nanotubes with the catalytic properties of iron or other metalated porphyrins may be of interest for CO₂ reduction [52,53] and small molecule activation [54,55].

3. Conclusion

Iron and copper/iron strapped porphyrins were combined with multiwalled carbon nanotubes and the electrocatalytic properties of the hybrids were investigated for the oxygen reduction reaction in alkaline media. The combination of nanotubes with the iron or copper/iron porphyrins systematically gave better catalytic ORR properties in terms of overpotential and current density than for the components taken separately. In particular, when the porphyrin inks were directly deposited on the glassy carbon electrode, a low efficiency was observed. This behavior is due to the lack of electrons available for the reduction of oxygen. In the catalyst ink, the porphyrins

are embedded in Nafion and only the molecules directly in contact with the glassy carbon disk can benefit from efficient electron transfers from the electrodes. The bimetallic porphyrin (Cu/Fe-P) exhibited slightly better ORR properties than the monometallic Fe-P. When carbon nanotubes were added, both the MWNT-Fe-P and MWNT-Cu/Fe-P hybrids were able to reduce oxygen *via* a four-electron pathway.

Acknowledgments

This work was supported by the JST-ANR grant ANR-14-JTIC-0002-01 (MECANO), the ANR grant ANR-16-CE29-0027-01 (MAGMA), a public grant overseen by the French National Research Agency as part of the “Investissements d’Avenir” program (Labex NanoSaclay, reference: ANR-10-LABX-0035), the CNRS, the Université de Strasbourg.

Supplementary data

Supporting information for this article is available on the journal's website under <https://doi.org/10.5802/crchim.86> or from the author.

References

- [1] F. Jaouen, E. Proietti, M. Lefèvre, R. Chenitz, J.-P. Dodelet, G. Wu, H. T. Chung, C. M. Johnston, P. Zelenay, *Energy Environ. Sci.*, 2011, **4**, 114.
- [2] A. Morozan, B. Jousselme, S. Palacin, *Energy Environ. Sci.*, 2011, **4**, 1238.
- [3] M. Shao, Q. Chang, J.-P. Dodelet, R. Chenitz, *Chem. Rev.*, 2016, **116**, 594.
- [4] Z. Chen, D. Higgins, A. Yu, L. Zhang, J. Zhang, *Energy Environ. Sci.*, 2011, **4**, 3167.
- [5] D.-W. Wang, D. Su, *Energy Environ. Sci.*, 2014, **7**, 576.
- [6] H. Wang, T. Maiyalagan, X. Wang, *ACS Catal.*, 2012, **2**, 781.
- [7] Q. Wei, X. Tong, G. Zhang, J. Qiao, Q. Gong, S. Sun, *Catalysts*, 2015, **5**, 1574.
- [8] J. H. Zagal, S. Griveau, J. F. Silva, T. Nyokong, F. Bedioui, *Coord. Chem. Rev.*, 2010, **254**, 2755.

- [9] M. A. Thorseth, C. E. Tornow, E. C. M. Tse, A. A. Gewirth, *Coord. Chem. Rev.*, 2013, **257**, 130.
- [10] W. He, Y. Wang, C. Jiang, L. Lu, *Chem. Soc. Rev.*, 2016, **45**, 2396.
- [11] A. Mahammed, Z. Gross, *Isr. J. Chem.*, 2016, **56**, 756.
- [12] W. Zhang, W. Lai, R. Cao, *Chem. Rev.*, 2017, **117**, 3717.
- [13] M. L. Pegis, C. F. Wise, D. J. Martin, J. M. Mayer, *Chem. Rev.*, 2018, **118**, 2340.
- [14] Y.-M. Zhao, G.-Q. Yu, F.-F. Wang, P.-J. Wei, J.-G. Liu, *Chem. Eur. J.*, 2019, **25**, 3726.
- [15] C. Zhang, W. Zhang, W. Zheng, *ChemElectroChem*, 2019, **11**, 655.
- [16] M. Liu, L. Wang, K. Zhao, S. Shi, Q. Shao, L. Zhang, X. Sun, Y. Zhao, J. Zhang, *Energy Environ. Sci.*, 2019, **12**, 2890.
- [17] U. I. Koslowski, I. Abs-Wurmbach, S. Fiechter, P. Bogdanoff, *J. Phys. Chem. C*, 2008, **112**, 15356.
- [18] U. I. Kramm, J. Herranz, N. Larouche, T. M. Arruda, M. L. Lefèvre, F. Jaouen, P. Bogdanoff, S. Fiechter *et al.*, *Phys. Chem. Chem. Phys.*, 2012, **14**, 11673.
- [19] A. Zitolo, V. Goelner, V. Armel, M.-T. Sougrati, T. Mineva, L. Stievano, E. Fonda, F. Jaouen, *Nat. Mater.*, 2015, **14**, 937.
- [20] T. Mineva, I. Matanovic, P. Atanassov, M.-T. Sougrati, L. Stievano, M. Clémancey, A. Kochem, J.-M. Latour, F. Jaouen, *ACS Catal.*, 2019, **9**, 9359.
- [21] R. Jasinski, *Nature*, 1964, **201**, 1212.
- [22] J. P. Collman, L. Fu, P. C. Herrmann, X. Zhang, *Science*, 1997, **275**, 949.
- [23] J. P. Collman, N. K. Devaraj, R. A. Decréau, Y. Yang, Y.-L. Yan, W. Ebina, T. A. Eberspacher, C. E. D. Chidsey, *Science*, 2007, **315**, 1565.
- [24] D. Ricard, B. Andrioletti, M. L'Her, B. Boitrel, *Chem. Commun.*, 1999, 1523.
- [25] F. Melin, A. Trivella, M. Lo, C. Ruzié, I. Hijazi, N. Oueslati, J. A. Wytko *et al.*, *J. Inorg. Biochem.*, 2012, **108**, 196.
- [26] J. P. Collman, S. Ghosh, *Inorg. Chem.*, 2010, **49**, 5798.
- [27] D. Ricard, A. Didier, M. L'Her, B. Boitrel, *Chem. Bio. Chem.*, 2001, **2**, 144.
- [28] D. Ricard, M. L'Her, P. Richard, B. Boitrel, *Chem. Eur. J.*, 2001, **7**, 3291.
- [29] D. K. Dogutan, S. A. Stoian, R. McGuire Jr., M. Schwalbe, T. S. Teets, D. G. Nocera, *J. Am. Chem. Soc.*, 2011, **133**, 131.
- [30] J. Rosenthal, D. G. Nocera, *Acc. Chem. Res.*, 2007, **40**, 543.
- [31] R. McGuire, D. K. Dogutan, T. S. Teets, J. Suntivich, Y. Shao-Horn, D. G. Nocera, *Chem. Sci.*, 2010, **1**, 411.
- [32] C. J. Chang, Z.-H. Loh, C. Shi, F. C. Anson, D. G. Nocera, *J. Am. Chem. Soc.*, 2004, **126**, 10013.
- [33] A. Morozan, S. Campidelli, A. Filoramo, B. Jusselme, S. Palacin, *Carbon*, 2011, **49**, 4839.
- [34] I. Hijazi, T. Bourgeteau, R. Cornut, A. Morozan, A. Filoramo, J. Leroy, V. Derycke, B. Jusselme, S. Campidelli, *J. Am. Chem. Soc.*, 2014, **136**, 6348.
- [35] N. Levy, A. Mahammed, M. Kosa, D. T. Major, Z. Gross, L. Elbaz, *Angew. Chem. Int. Ed.*, 2015, **54**, 14080.
- [36] A. Friedman, L. Landau, S. Gonen, Z. Gross, L. Elbaz, *ACS Catal.*, 2018, **8**, 5024.
- [37] M. L. Rigsby, D. J. Wasylenko, M. L. Pegis, J. M. Mayer, *J. Am. Chem. Soc.*, 2015, **137**, 4296.
- [38] X. Wang, B. Wang, J. Zhong, F. Zhao, N. Han, W. Huang, M. Zeng, J. Fan, Y. Li, *Nano Res.*, 2016, **9**, 1497.
- [39] H. Jia, Z. Sun, D. Jiang, S. Yang, P. Du, *Inorg. Chem. Front.*, 2016, **3**, 821.
- [40] M. Hanana, H. Arcostanzo, P. K. Das, M. Bouget, S. Le Gac, H. Okuno, R. Cornut *et al.*, *New J. Chem.*, 2018, **42**, 19749.
- [41] B. Boitrel, M. Bouget, P. K. Das, S. Le Gac, T. Roisnel, M. Hanana, H. Arcostanzo, R. Cornut *et al.*, *J. Porphyr. Phthalocyanines*, 2020, **24**, 675.
- [42] C. Kahlfuss, J. A. Wytko, J. Weiss, *ChemPlusChem*, 2017, **82**, 584.
- [43] P. Vorburger, M. Lo, S. Choua, M. Bernard, F. Melin, N. Oueslati, C. Boudon *et al.*, *Inorg. Chim. Acta*, 2017, **468**, 232.
- [44] M. Koepf, F. Melin, J. Jaillard, J. Weiss, *Tetrahedron Lett.*, 2005, **46**, 139.
- [45] J.-P. Tessonier, D. Rosenthal, T. W. Hansen, C. Hess, M. E. Schuster, R. Blume *et al.*, *Carbon*, 2009, **47**, 1779.
- [46] M. Lo, D. Mahajan, J. A. Wytko, C. Boudon, J. Weiss, *Org. Lett.*, 2009, **11**, 2487.
- [47] X. Lu, L. Dai, *Nat. Rev. Mater.*, 2016, **1**, article no. 16064.
- [48] J. H. Espenson, R. J. Christensen, *Inorg. Chem.*, 1977, **16**, 2561.
- [49] J. A. R. van Veen, H. A. Colijn, *Ber. Bunsenges. Phys. Chem.*, 1981, **85**, 700.
- [50] D. Banham, S. Ye, K. Pei, J.-I. Ozaki, T. Kishimoto, Y. Imashiro, *J. Power Sources*, 2015, **285**, 334.
- [51] F. Melin, C. Boudon, M. Lo, K. J. Schenk, M. Bonin, P. Ochsenbein, M. Gross, J. Weiss, *J. Porphyr. Phthalocyanines*, 2007, **11**, 212.
- [52] C. Costentin, S. Drouet, M. Robert, J.-M. Savéant, *Science*, 2012, **338**, 90.
- [53] C. Costentin, J.-M. Savéant, *Nat. Rev. Chem.*, 2017, **1**, article no. 0087.
- [54] E. Anxolabéhère-Mallart, J. Bonin, C. Fave, M. Robert, *Dalton Trans.*, 2019, **48**, 5869.
- [55] S. J. Thompson, M. R. Brennan, S. Y. Lee, G. Dong, *Chem. Soc. Rev.*, 2018, **47**, 929.